

## Nonequilibrium Dynamics in a Superconducting Thin-Film Microbridge

Robert A. Peters

*Catholic University of America, Washington, D. C. 20064*

and

Frederic J. Rachford<sup>(a)</sup> and Stuart A. Wolf*Naval Research Laboratory, Washington, D. C. 20375*

(Received 12 September 1977)

First measurements of the time for the recovery of the critical current at a phase-slip site have been made by studying the frequency dependence of the hysteretic rf current-voltage characteristics in the low-power limit. The data are incompatible with recent hot-spot models but can be explained by a model relating a nonequilibrium length to the critical current.

The production and decay of nonequilibrium states in superconductors is currently of great interest. In recent studies, nonequilibrium states have been produced by tunneling,<sup>1</sup> laser excitation,<sup>2</sup> thermal phonon injection,<sup>3</sup> ultrasonic phonons,<sup>4</sup> conversion of normal currents to supercurrents at superconducting boundaries,<sup>5</sup> rapid variation of the supercurrent,<sup>6</sup> etc. Here, we report the first determination of the temporal response of the nonequilibrium state generated by the phase-slip process at a site in an ultrathin-film superconducting microbridge in an rf SQUID (superconducting quantum interference device) configuration.

Our data were obtained using a broadband, continuously variable, nonresonant mutual inductance bridge (5 MHz–1.8 GHz), a conventional 20-MHz tuned circuit, and a 9.2-GHz spectrometer employing a resonant cavity.

In order to minimize heating effects, we investigated numerous thin-film cylindrical SQUID's at 20 MHz and 9.2 GHz and selected a very low-critical-current niobium sample. This sample allowed us to study the hysteretic response over a wide temperature range with minimal heating. The physical dimensions of this niobium weak link are 3  $\mu\text{m}$  in the direction of current flow, 40  $\mu\text{m}$  wide, and 35  $\text{\AA}$  thick, totally covered by a 600- $\text{\AA}$  insulating oxide layer. This sample has a superconducting critical temperature of 2.8 K. Consistent results were obtained with the sample immersed in liquid helium (both above and below the  $\lambda$  point) and with the sample cooled by helium exchange gas.

Inset (b) of Fig. 1 illustrates the relation between the detected rf voltage amplitude and the applied rf current amplitude for various frequencies at 2.167 K as observed with the broadband system. The temperature dependence of the crit-

ical current can be described in terms of a mean-field behavior and is independent of frequency. This mean-field dependence is indicative of a current distribution which is relatively uniform over the width of the microbridge. Above a frequency of 120 MHz hysteresis develops in the critical currents. That is, dissipation persists in the weak link below the mean-field critical current,  $I_t$ , until a sudden return to the uniform superconducting state occurs at  $I_t(f)$ . This critical-current hysteresis is similar to that observed by Skocpol, Beasley, and Tinkham<sup>7,8</sup> in the dc  $I$ - $V$  characteristics of tin microbridges and by Rachford *et al.*<sup>9</sup> in the 9.2-GHz microwave response of weak links of various geometries and materi-

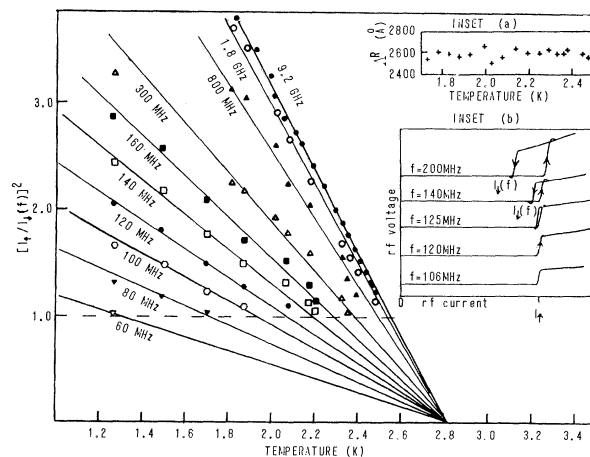


FIG. 1.  $[I_c/I_t(f)]^2$  obtained from data such as shown in inset (b) is plotted vs temperature. Inset (a) shows the temperature independence of the half-length,  $\Lambda^R$ , of the dissipative region as inferred from the 9.2-GHz dissipation measurements. Inset (b) shows the observed development of hysteresis in the detected rf voltage amplitude vs applied rf current amplitude as frequency is increased.

als.

In Fig. 1, measured values of  $[I_{\uparrow}/I_{\downarrow}(f)]^2$  are plotted as a function of temperature at various frequencies. Note that at each frequency this ratio can be represented by straight lines extrapolating to zero at a single temperature ( $T_c$  of the sample) and, hence, there is a temperature-dependent frequency for the onset of the hysteresis  $[I_{\uparrow}/I_{\downarrow}(f) = 1]$ . Figure 2 is a plot of the slopes of these linear fits versus frequency of observation and shows a limiting value at higher frequencies. A viable model to explain the hysteresis must predict the features depicted in Figs. 1 and 2.

An rf voltage will be detected when the instantaneous current exceeds the critical current in the sample. Initially the critical current,  $I_{\uparrow}$ , is given by the mean-field value. Once phase-slip processes start at a site in the sample, disequilibrium effects may lower the instantaneous critical current. When the instantaneous rf current becomes less than the depressed critical current, the critical current will recover towards its mean-field value. The critical current on a subsequent rf half-cycle is a function of the rf period. Thus the hysteresis is frequency dependent

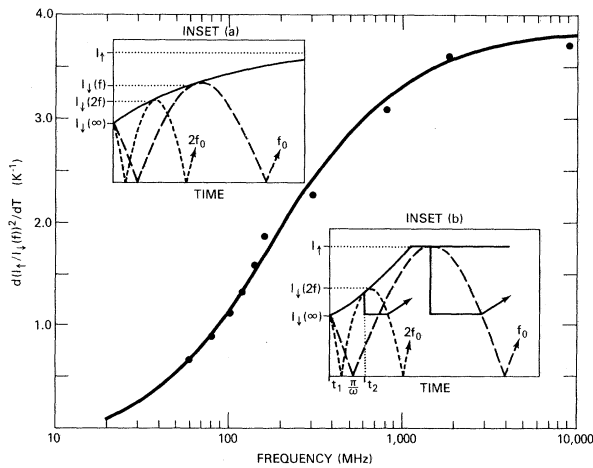


FIG. 2. The slopes,  $d[I_{\uparrow}/I_{\downarrow}(f)]^2/dT$ , from the previous figure are plotted vs frequency (solid circles). The solid curve is calculated from the  $\Lambda$  model (see text) with  $\tau_d = 5.5$  nsec and  $(I_{\uparrow}/I_{\downarrow})^2 = 3.87$ . The recovery of the critical current (solid curve) vs time for the hot-spot and the  $\Lambda$  models are, respectively, plotted in insets (a) and (b). The rectified, instantaneous rf currents at two frequencies,  $f_0$  and  $2f_0$ , are drawn with amplitudes just sufficient to intersect the recovering critical currents. In inset (a),  $I_{\uparrow}(f) < I_{\downarrow}$  resulting in hysteresis at both (all) frequencies. In inset (b), only the higher frequency results in hysteresis.

and reflects the recovery process.

A hot-spot model has been used to explain hysteresis.<sup>7,10</sup> This heating model predicts an asymptotic recovery of the instantaneous critical current toward the mean-field value. We approximate this asymptotic recovery by the exponential curve in inset (a) of Fig. 2. In this inset, the rectified, instantaneous rf currents at two frequencies are indicated with the minimum amplitudes  $I_{\downarrow}(f_0)$  and  $I_{\downarrow}(2f_0)$  sufficient to intersect the recovering critical current and to sustain the heating cyclically. It can be inferred from such curves that hysteresis will be present at *all* frequencies due to the asymptotic recovery of the critical current towards the mean-field value. Only the magnitude, and not the onset, of hysteresis will depend on frequency. Furthermore, when  $I_{\uparrow}$  is given by the mean-field temperature dependence, the hot-spot model does not predict linear curves of  $[I_{\uparrow}/I_{\downarrow}(f)]^2$  versus temperature. Such curves also are predicted to converge at or very near the point  $[I_{\uparrow}/I_{\downarrow}(f)]^2 = 1$  rather than at zero as observed in Fig. 1. Detailed computer simulations of the hot-spot model have been carried out and are consistent with these qualitative conclusions. For these three reasons, the data are incompatible with the hot-spot model.

Tinkham<sup>11</sup> has proposed a model expected to apply where "simple" heating can be ignored. In this model (here called the  $\Lambda$  model), the instantaneous critical current is given by  $I_c \propto |\Psi|^2 \pi / 2L$ , where  $L$  is a characteristic length for variation of the order parameter,  $\Psi$ . The usual mean-field dependence is obtained with  $L = (\sqrt{3}\pi/2)\xi(T)$ . If nonequilibrium processes cause  $\Psi$  to vary over a length scale greater than the coherence length,  $\xi$ , the critical current will be reduced from  $I_c \propto |\Psi|^2 / \xi(T) \sqrt{3}$  to  $I_c \propto |\Psi|^2 \pi / 2\Lambda$ . In steady state, the length  $\Lambda$  has been identified with the Pippard "quasiparticle diffusion distance,"  $\Lambda_0 = (lv_F \tau_s / 3)^{1/2}$ , where  $l$  is the elastic scattering length,  $v_F$  is the Fermi velocity, and  $\tau_s$  is the appropriate inelastic scattering time.<sup>8</sup> The ratio of the squares of the undisturbed mean-field critical current,  $I_{\uparrow}$ , to the depressed value,  $I_{\downarrow}$ , is given by

$$(I_{\uparrow}/I_{\downarrow})^2 = [2\Lambda/\pi\xi(0)\sqrt{3}]^2 (T - T_c)/T_c. \quad (1)$$

In a recent paper, Smith<sup>12</sup> has shown that excess quasiparticles produced by optical illumination in a superconducting film will produce a spatial instability on a scale governed by the quasiparticle diffusion distance  $\Lambda_0$ . The quasiparticles will depress the local superconducting

gap and will be trapped in the resulting gap well by Andreev reflections. If quasiparticle production is stopped, the inhomogeneity will relax back to the uniform superconducting state.

In our samples, quasiparticles are produced in bursts by the phase-slip process and are sustained by normal dissipation while the instantaneous rf current level exceeds the critical current. We expect that a Smith-type gap inhomogeneity will be produced and will relax during part of the rf cycle when the current amplitude is subcritical.

Constructing a simple model, we approximate the decay of the nonequilibrium length,  $\Lambda$ , by  $\Lambda = \Lambda_0 \exp(-t/\tau_d)$ , where  $\Lambda_0$  and  $\tau_d$  are assumed to be temperature independent. The depressed critical current then recovers as  $\exp(+t/\tau_d)$  until  $\Lambda$  becomes comparable to  $\xi$  and  $I_c$  abruptly stops decreasing at the mean-field value  $I_\dagger$ . We also assume that the gap inhomogeneity is established in a time short in comparison to the decay time and the rf period. The minimum rf amplitude,  $I_\dagger(f)$ , necessary to sustain cyclically the dissipative state at the phase-slip site occurs when the critical current (growing in time as  $\Lambda$  relaxes) *tangentially* meets the instantaneous rf current at time  $t_2$  [see Fig. 2, inset (b)]. With this condition and the above assumptions,  $t_1$ , the time for the start of the recovery of the instantaneous critical current, can be iteratively computed using  $t_1 = t_2 - \tau_d \ln |\sin \omega t_2 / \sin \omega t_1|$ , where  $t_2$  is given by  $t_2 = (\tan^{-1} \omega \tau_d) / \omega$ . Once we have found  $t_1$ , the value of  $I_\dagger(f) / I_\dagger$  can easily be obtained, where  $I_\dagger$  is now taken to represent the saturated, high-frequency value of the reduced critical current,  $I_\dagger(\infty)$ .

In this model, the depressed critical current reverts to the mean-field value when the instability length nears the temperature-dependent coherence length. This nonasymptotic recovery distinguishes it from the heating model and predicts a temperature-dependent frequency for the onset of hysteresis. From Eq. (1), the plots of  $[I_\dagger / I_\dagger(f)]^2$  versus temperature should be linear and converge to zero at  $T_c$ , in agreement with the experimental data (see Fig. 1).

Quantitative predictions of this model, shown by the solid curve in Fig. 2, are in excellent agreement with the experimental points (solid circles). Two parameters were used in obtaining the solid curve, the ratio  $[I_\dagger / I_\dagger]^2 = 3.87$  and the time  $\tau_d = 5.5$  nsec.<sup>13</sup> The shape of the curve is determined from the model itself. By Eq. (1),  $\Lambda_0 / \xi(0) = 9.0$ .

Estimating  $\xi(0)$  from the expression  $\xi(0)$

$= 0.85(0.18 l \hbar v_F / k_B T_c)^{1/2}$  where  $l = 35 \text{ \AA}$ ,  $v_F = 0.68 \times 10^8 \text{ cm/sec}$ , and  $T_c = 2.83 \text{ K}$ , we find  $\Lambda_0 = 2600 \text{ \AA}$ , and from  $\Lambda_0 = (l v_F \tau_s / 3)^{1/2}$ , we find a quasiparticle inelastic scattering time  $\tau_s = 8.5 \times 10^{-11}$  sec. Since it typically takes a time  $\tau_s$  for quasiparticles created in the initial phase slip to diffuse out a distance  $\Lambda_0$ , we expect that  $\tau_s$  determines the time for the establishment of the quasiparticle distribution, whereas  $\tau_d$  is the time for the relaxation of the nonequilibrium state involving the interaction of quasiparticles,  $2\Delta$  phonons, and pairs.

In the high-frequency limit we explicitly consider the effects of a finite buildup time,  $\tau_s$ , for the establishment of the nonequilibrium length. Consider the process where bursts of quasiparticles are created (at the phase-slip site) on each half of an rf cycle. These quasiparticles continue to diffuse outward even between  $t_1$  and  $t_2$  (Fig. 2, inset b). Thus even at high frequencies  $\Lambda$  will build up to nearly its saturated value after  $\sim \omega \tau_s$  cycles provided  $\tau_s \ll \tau_d$ , as is the case with this sample. Thus the high-frequency predictions which neglect  $\tau_s$  are only slightly modified. In fact, numerical solutions using the measured values of  $\tau_s$  and  $\tau_d$  cannot be distinguished from the solid line in Fig. 2.

Previously, the diffusion length has been estimated from the differential resistance obtained from the dc  $I$ - $V$  characteristics of superconducting microbridges.<sup>8</sup> Similarly, the 9.2-GHz loss characteristics of this sample yield a differential resistance and an estimate of  $\Lambda$ , independent of the presence of hysteresis. Inset (a) of Fig. 1 shows that the 9.2-GHz resistive diffusion length,  $\Lambda^R$ , is independent of temperature, and is in excellent agreement with  $\Lambda_0$  predicted by the  $\Lambda$  model.

In these experiments, the phase-slip process is synchronized with the rf cycle, whereas in dc  $I$ - $V$  experiments, phase slip proceeds at the Josephson frequency. In the latter case under typical conditions the Josephson period is short with respect to  $\tau_d$  and the extracted  $\Lambda$  is constant, corresponding to the high-frequency regime of Fig. 2. However, if the critical current is small, the voltage across the site may produce Josephson oscillations with a period of the order of  $\tau_d$ , resulting in an apparent voltage- (frequency-) dependent  $\Lambda$ . This effect may be related to the "feet" observed in the dc  $I$ - $V$  characteristics at low currents.<sup>14</sup>

In summary, the frequency and temperature dependence of critical-current hysteresis in ultra-

thin-film niobium samples, which cannot be adequately described by the hot-spot theory, has been described in terms of the "healing" of a quasiparticle-induced gap inhomogeneity.

We acknowledge the support of the U. S. Office of Naval Research, the Research Corporation, and the National Science Foundation and the loan of a Varian E12 system from the Army Night Vision Laboratory, Ft. Belvoir, Virginia. We would like to thank Dr. Martin Nisenoff and Professor Jack Leibowitz for their initial advice and encouragement in this project. We also wish to thank Mr. Talat Refai for his help with computer calculations and Mr. James Kennedy for sample preparation.

<sup>(a)</sup>Present address: Laboratory for High Pressure Science, Dept. of Chemical Engineering, University of Maryland, College Park, Md. 20742.

<sup>1</sup>See S. B. Kaplan, J. R. Kirtley, and D. N. Langenberg, *Phys. Rev. Lett.* **39**, 291 (1977), for references.

<sup>2</sup>G. A. Sai-Halasz, C. C. Chi, A. Denenstein, and D. N. Langenberg, *Phys. Rev. Lett.* **33**, 215 (1974); P. Hu, R. C. Dynes, V. Narayanamurti, H. Smith, and W. F. Brinkman, *Phys. Rev. Lett.* **38**, 361 (1977); I. Schuller and K. E. Gray, *Phys. Rev. Lett.* **36**, 429 (1976).

<sup>3</sup>T. Wong, J. T. C. Yeh, and D. N. Langenberg, *IEEE*

*Trans. Mag.* **13**, 743 (1977).

<sup>4</sup>J. R. Leibowitz and M. C. Wilt, *Phys. Rev. Lett.* **38**, 1167 (1977); T. R. Tredwell and E. H. Jacobsen, *Phys. Rev. B* **13**, 2931 (1976).

<sup>5</sup>M. L. Yu and J. E. Mercereau, *Phys. Rev. B* **12**, 4909 (1975).

<sup>6</sup>R. A. Peters and H. Meissner, *Phys. Rev. Lett.* **30**, 965 (1973); T. Kommers and J. Clarke, *Phys. Rev. Lett.* **38**, 1091 (1977); J. C. Amato and W. L. McLean, *Phys. Rev. Lett.* **37**, 930 (1976).

<sup>7</sup>W. J. Skocpol, M. R. Beasley, and M. Tinkham, *J. Appl. Phys.* **45**, 4054 (1974).

<sup>8</sup>W. J. Skocpol, M. R. Beasley, and M. Tinkham, *J. Low Temp. Phys.* **16**, 145 (1974).

<sup>9</sup>F. J. Rachford, S. A. Wolf, J. K. Hirvonen, J. Kennedy, and M. Nisenoff, *IEEE Trans. Mag.* **13**, 875 (1977); F. J. Rachford, C. Y. Huang, S. A. Wolf, and M. Nisenoff, *Solid State Commun.* **17**, 1493 (1975); F. J. Rachford, Ph.D. thesis, Case Western Reserve University, Cleveland, Ohio, 1975 (unpublished).

<sup>10</sup>S. K. Decker and D. W. Palmer, *J. Appl. Phys.* **48**, 2043 (1977); T. M. Klapwijk, M. Sepers, and J. E. Mooij, *J. Low Temp. Phys.* **27**, 801 (1977); R. P. Heubener, *J. Appl. Phys.* **46**, 4982 (1975).

<sup>11</sup>M. Tinkham, private communication.

<sup>12</sup>L. N. Smith, *J. Low Temp. Phys.* **28**, 519 (1977).

<sup>13</sup>It is interesting to note that  $\tau_d$  is nearly equal to  $\tau_F = 6.2$  nsec, the scattering time for electrons at the Fermi surface at  $T_c = 2.83$  and Debye temperature,  $\theta_D = 275$  K (Ref. 8).

<sup>14</sup>M. Octavio, W. J. Skocpol, and M. Tinkham, to be published.

## Divalent Surface State on Metallic Samarium

G. K. Wertheim and G. Crecelius<sup>(a)</sup>

*Bell Laboratories, Murray Hill, New Jersey 07974*

(Received 13 January 1978)

It is shown that the first atomic layer of trivalent metallic samarium has a large divalent component. The valence transition is attributed to a narrowing of the  $5d$  band which populates the low-lying  $4f^6$  state.

The existence of a unique, resolvable signal from the first layer of atoms in core-level spectroscopies has long been anticipated but never successfully demonstrated.<sup>1,2</sup> On the other hand, surface states have been identified in many photoemission experiments.<sup>3</sup> We report here the first example, metallic samarium, in which a spectrum of surface atoms has been resolved and identified in photoemission from both core and valence states. The detection was made possible by a valence transition at the surface.

The fact that a divalent signal appears in the

spectra of Sm metal has recently been pointed out,<sup>4</sup> but the question of whether it is a bulk or surface phenomenon was left open. The initial identification was made in the  $4d$  spectrum, on the basis of comparisons with the spectra of trivalent SmSb, divalent SmTe, and intermediate-valence SmB<sub>6</sub>. The overlap between the 2+ and 3+ spectra, as well as the complex multiplet structures make the  $4d$  spectrum less attractive for detailed analysis than the simpler  $3d$  spectra. It is well known, however, that the  $3d$  spectra of insulating compounds of La, Ce, Pr, and Nd have